

N72-11897

**NASA TECHNICAL
MEMORANDUM**

NASA TM X-67905

NASA TM X-67905

**CASE FILE
COPY**

**APPLICATION OF QUADRATIC OPTIMIZATION
TO SUPERSONIC INLET CONTROL**

by Bruce Lehtinen and John R. Zeller
Lewis Research Center
Cleveland, Ohio

TECHNICAL PAPER proposed for presentation at
Fifth Congress of the International Federation of Automatic Control
Paris, France, June 12-17, 1972

APPLICATION OF QUADRATIC OPTIMIZATION TO SUPERSONIC INLET CONTROL

Bruce Lehtinen* and John R. Zeller*
National Aeronautics and Space Administration
Lewis Research Center
Cleveland, Ohio

ABSTRACT

This paper describes the application of linear stochastic optimal control theory to the design of the control system for the air intake (inlet) of a supersonic air-breathing propulsion system. The controls must maintain a stable inlet shock position in the presence of random airflow disturbances and prevent inlet unstart. Two different linear time invariant control systems are developed. One is designed to minimize a nonquadratic index, the expected frequency of inlet unstart, and the other is designed to minimize the mean square value of inlet shock motion. The quadratic equivalence principle is used to obtain the best linear controller that minimizes the nonquadratic performance index. The two systems are compared on the basis of unstart prevention, control effort requirements, and sensitivity to parameter variations. It is concluded that while controls designed to minimize unstarts are desirable in that the index minimized is a physically meaningful quantity, computation time required is longer than for the minimum mean square shock position approach. In addition, the simpler minimum mean square shock position solution produced expected unstart frequency figures which were not significantly worse than those of the nonquadratic solution.

I INTRODUCTION

The purpose of this paper is to study two approaches to supersonic inlet control system design. Both approaches are similar in that they use optimal control theory, however each uses a different performance criterion. The overall goal is to provide a more rational and unified approach to inlet control design.

A supersonic inlet is that portion of a supersonic propulsion system which decelerates air from supersonic velocity (ahead of the aircraft) to subsonic velocity (at the entrance to the compressor). This deceleration is needed because present compressors require air at subsonic velocity. An inlet is a critical part of a supersonic propulsion system. This is not the case for an inlet on a subsonic aircraft. This is because the dynamic head is large at high supersonic Mach

numbers and may comprise a large percentage of the overall engine compression. For subsonic propulsion systems, however, almost all the compression is done by the engine's compressor. To aid the supersonic inlet in operating at peak efficiency in the face of varying flight conditions, certain variable geometry features, and associated controls, are required.

A typical axisymmetric supersonic inlet is shown in Fig. 1 in a normal operating configuration. Air at supersonic velocity enters the inlet past a weak oblique shock wave. It is compressed supersonically past a minimum area point, or throat, up to the terminal normal shock. Thereafter, the flow is subsonic up to the compressor face station.

A stable operating condition for the inlet is one in which the throat Mach number is greater than one and the normal shock is downstream of the throat. This is the so-called started condition. An upstream or downstream flow disturbance may, however, cause the throat Mach number to drop to one, or it may cause the normal shock to move ahead of the throat. When either of these occur, the inlet unstarts and enters an undesirable, unstable operating region (called unstart).

During an unstart a shock wave sweeps out of the throat and a strong shock wave forms ahead of the inlet. The result is a large increase in drag and a large decrease in the pressure recovered at the compressor face. In addition there may exist an oscillatory flow pattern within the inlet. Aircraft performance under these conditions is poor and often unacceptable. Thus, unstart is very undesirable.

In order to prevent unstart and to maintain the desired operation of the inlet, two basic control modes are required. The first, shown in Fig. 1, is a translating centerbody. A forward translation of the centerbody causes the throat area to increase. By varying the centerbody position, the throat area can be varied so that the throat Mach number can be kept above one, even if the free stream Mach number decreases. The second manipulated variable is bypass door opening. Bypass doors are controlled to dump excess air in case a

*Aerospace Engineer.

disturbance causes a pressure rise at the compressor face. By spilling excess air, the pressure disturbance is prevented from pushing the normal shock forward ahead of the throat.

Primary inlet disturbances can occur either upstream or downstream of the inlet. Upstream disturbances may result from such things as shock waves from passing aircraft or atmospheric turbulence. Turbulence may consist of pressure, temperature or velocity (gusts) changes. Downstream disturbances may be due to changes in engine air flow demand which results from a pilot induced throttle change. Also aerodynamic noise may be generated by the compressor, or combustion noise may get fed back to the compressor face in duct burning fan type engines. The overall control design goals are: (1) to keep the throat Mach number and shock position as close as possible to their unstart limits. This maximizes efficiency. (2) to keep the deviations of throat Mach number and shock position small so as to prevent unstart. (3) to design a control which produces desired results while using a reasonable amount of control power.

II PRESENT INLET CONTROL DESIGN TECHNIQUES

Much of the work that has been done on inlet control has been devoted towards modelling and simulation. Walitt⁽¹⁾ developed a Helmholtz resonator model for a mixed-compression inlet. Willoh⁽²⁾ derived a linearized, small perturbation, high frequency model for an axisymmetric inlet. Mays⁽³⁾ developed a nonlinear, large perturbation, low frequency model. All of the above approaches have been used in combination with test data to provide inlet control models.

Controls development includes work done by Chun and Burr⁽⁴⁾ and Crosby, Neiner, and Cole.⁽⁵⁾ Designs for both of the aforementioned controls were obtained using frequency domain techniques. Barry⁽⁶⁾ conducted a design study based on an explicit description of inlet disturbances. The disturbance he treated was atmospheric turbulence, described by experimentally determined power spectral densities and probability distributions. Barry's criterion for evaluating inlet controls was the expected frequency of unstart. This criterion, borrowed from the field of structural design, proved quite applicable to inlet control and provided a meaningful criterion for judging control effectiveness. Basically, it gives the designer a more rational basis (as opposed to frequency response methods) of judging inlet control systems.

In a previous work,⁽⁷⁾ the authors extended Barry's work to the design of optimal inlet controls which minimize the expected frequency of unstarts. This paper extends that work to a more realistic case in which actuator dynamics and nonwhite disturbances are included, as well as a comparison of alternate performance indices. Using a linearized operating point model, the present study compares and contrasts controls resulting from the minimization of two performance indices. The first index is the mean square value of shock position. The second is the expected frequency of inlet unstarts (as was used in ref. 6).

The following sections of the paper are outlined as follows: Section III discusses the particular, somewhat restricted, optimal control problem considered. The next section is an outline of linear quadratic optimal control and estimation theory and the application of this theory to nonquadratic performance indexes. Section V describes the computer algorithms used followed by section VI in which state variable inlet models and disturbance descriptions are presented. The results of a control study comparing and contrasting controllers for each index are presented in section VII.

III OPTIMAL INLET CONTROL

The problem considered is not the complete inlet control problem with two degrees of control freedom but rather is restricted to single-input, single-output control. This case is shown in Fig. 2 where the single control input is bypass door command and the one measurable output is throat exit static pressure (P_{te}). This is a pressure measured just downstream of the normal shock. The control is designed to take care of downstream disturbances only. Disturbances are considered to be random with a Gaussian probability distribution.

In Fig. 2, the G's represent transfer functions for the system dynamics, linearized about an operating point. GCONTROL is the optimal controller, designed to control y_s (shock position). Note that y_s cannot be directly measured. Instead, the pressure P_{te} is used. P_{te} has been found to be related to shock position through shock position dynamics GSHOCK. The additional transfer functions on Fig. 2 represent bypass door dynamics GBDP and noise coloring GCOLOR. Noise coloring accounts for the fact that the random disturbance at the compressor face is not in general white noise. Also shown in the figure is measurement noise on the signal P_{te} . This measurement noise is assumed white.

A design constraint selected at the outset was that the control should be linear and time invariant. This is desirable first of all for simplicity. Secondly, linear time invariant control provides consistency to the analysis (Gaussian signals through linear systems remain Gaussian). Also, and most important, linear optimal control theory results can be used.

The first of the design approaches taken is to minimize a quadratic performance index. This index can be written as

$$J_q = \sigma_{y_s}^2 + k\sigma_{u_b}^2 \quad (1)$$

where the σ^2 terms are mean square values and k is a constant weighting parameter. Minimizing J_q minimizes the weighted sum of mean square shock position and bypass door command. The problem of minimizing J_q for a linear system is a classical linear quadratic problem.

For the second approach a nonquadratic performance index was chosen to be minimized. This was given as

$$J_{nq} = \lambda + k\sigma_{u_p}^2 \quad (2)$$

where

$$\lambda = \frac{1}{2\pi} \sqrt{\frac{\sigma_y^2}{\sigma_y^2}} \exp\left(\frac{-\alpha^2}{2\sigma_y^2}\right)$$

Lambda is the expected frequency of unstarts, α is the shock position tolerance, and σ^2 's are mean square values. This is a classic exceedance equation and was used by Barry.⁽⁶⁾ Due to the non-quadratic nature of J_{nq} the standard linear quadratic results cannot be used directly. In this paper a desired linear time invariant control minimizing J_{nq} was found using the quadratic equivalence principle. This technique was developed by Skelton⁽⁹⁾ and applied to launch booster control system design. Use of the principle will be discussed in more detail in section IV. Quadratic equivalence allows use of the same computer programs which are used in solving the problem of minimizing J_q . The result obtained is the best linear control which causes the expected frequency of unstarts to be a minimum for a given amount of control effort.

IV OPTIMAL CONTROL THEORY

The approaches to the inlet control design problem just described make use of the known results of the linear stochastic optimal control and estimation problem (Bryson and Ho, ref. 8). The problem and solution can be summarized as follows:

Given a time invariant plant described by

$$\dot{x} = Ax + Bu + Dw \quad (3)$$

with measurement vector

$$z = Hx + v \quad (4)$$

and output vector

$$y = Cx \quad (5)$$

x is the state vector, u the control vector and w and v are white Gaussian plant and measurement noise vectors. Plant and measurement noise correlation matrices are given by

$$\left. \begin{aligned} E\{w(t)w^T(t+\tau)\} &= Q\delta(\tau) \\ E\{v(t)v^T(t+\tau)\} &= R\delta(\tau) \end{aligned} \right\} \quad (6)$$

The problem is to minimize the quadratic performance index

$$J = E\{1/2(x^T Q_c x + 2x^T N u + u^T P_c u)\} \quad (7)$$

Equations (3) to (7) define the time invariant form of the linear stochastic optimal control and estimation problem. The solution is

$$u = -K_c \hat{x} \quad (8)$$

where the state estimate \hat{x} is generated by a

Kalman filter whose differential equation is

$$\dot{\hat{x}} = A\hat{x} + Bu + K_e(z - H\hat{x}) \quad (9)$$

Control gain matrix K_c is

$$K_c = P_c^{-1}(B^T S + N^T) \quad (10)$$

where S is the solution to the steady-state Riccati equation

$$S(A - B P_c^{-1} N^T) + (A - B P_c^{-1} N^T)^T S - S(B P_c^{-1} B^T) S + (Q_c - N P_c^{-1} N^T) = 0 \quad (11)$$

Kalman filter gains are given by

$$K_e = P H^T R^{-1} \quad (12)$$

where P is the covariance of the estimation error and is the solution to

$$AP + P A^T - P(H^T R^{-1} H)P + D Q D^T = 0 \quad (13)$$

If the error in the estimate is defined as

$$e \triangleq \hat{x} - x \quad (14)$$

then the covariance matrices of x , \hat{x} , and e can be related by

$$X = E\{xx^T\} = E\{(\hat{x} - e)(\hat{x} - e)^T\} = \hat{X} + P \quad (15)$$

As shown in Bryson, the covariance of \hat{x} , \hat{X} , is given by the solution to the following Lyapunov equation

$$(A - BK_c)\hat{X} + \hat{X}(A - BK_c)^T + P(H^T R^{-1} H)P = 0 \quad (16)$$

By adding Eqs. (13) and (16), a similar Lyapunov equation,

$$(A - BK_c)X + X(A - BK_c)^T + (BK_c)P + P(BK_c)^T + D Q D^T = 0 \quad (17)$$

is obtained, which can be solved for the state covariance matrix X . Control gains K_c and Kalman filter gains K_e define the optimal controller. The state covariance matrix X contains mean square state information, which is needed for overall system evaluation.

Inlet Problem - Quadratic Performance Index

Turning now to the particular case of interest, the inlet problem, the following scalar quantities are defined: $u \triangleq u_p$, $w \triangleq w_w$, and $y \triangleq y_s$. For the quadratic problem, it is desired that J_q (eq. (1)) be minimized. It is a simple matter to write J_q in form of the general quadratic index of Eq. (7). Since

$$\sigma_{y_s}^2 = E\{y_s^2\} = E\{x^T(C^T C)x\} \quad (18)$$

and

$$\left. \begin{aligned} k\sigma_{u_b}^2 &= E\{ku_b^2\}, \text{ setting} \\ Q_c &= C^T C \\ N &= 0 \\ P_c &= k \end{aligned} \right\} \quad (18a)$$

allows the quadratic inlet problem to be solved using the solution given by Eqs. (8) to (17).

Inlet Problem - Nonquadratic Performance Index

Whereas the quadratic case of minimizing shock position can be solved in a straight forward manner, minimizing J_{nq} (eq. (2)) requires some additional considerations. In this paper the quadratic equivalence principle will be used to convert the nonquadratic problem into an equivalent quadratic one. For a discussion of quadratic equivalence, the reader is referred to Ref. 9.

The necessary condition for existence of a stationary point of J_{nq} is that $\delta(J_{nq}) = 0$. Thus Eq. (2) becomes

$$\delta(J_{nq}) = \delta(\lambda) + k\delta(\sigma_{u_b}^2) \quad (19)$$

Expanding Eq. (19) in terms of $\sigma_{y_s}^2$, $\sigma_{y_s}^2$, and $\sigma_{u_b}^2$, one obtains

$$0 = \delta(\sigma_{y_s}^2) + W_1 \delta(\sigma_{y_s}^2) + W_2 \delta(\sigma_{u_b}^2) \quad (20)$$

where parameters W_1 and W_2 are given by

$$\left. \begin{aligned} W_1 &= \frac{\sigma_{y_s}^2}{\sigma_{y_s}^2} \left(\frac{\alpha^2}{\sigma_{y_s}^2} - 1 \right) \\ W_2 &= 4\pi k \sigma_{y_s} \sigma_{y_s} \exp\left(\frac{\alpha^2}{2\sigma_{y_s}^2}\right) \end{aligned} \right\} \quad (21)$$

The quadratic equivalence principle states that two performance indices (one quadratic, one nonquadratic) are equivalent if their first variations are equal. This leads to the conclusion that the control designed via quadratic equivalence is the best linear control that minimizes the nonquadratic performance index.

In order to use the quadratic equivalence principle in the case under discussion, the variation of the quadratic performance index, J (eq. (7)), is set equal to zero, giving:

$$\delta(E\{x^T Q_c x\}) + 2\delta(E\{x^T Nu\}) + \delta(E\{u^T P_c u\}) = 0 \quad (22)$$

To determine the conditions under which $\delta(J) = \delta(J_{nq})$, it is necessary to expand Eq. (20) in terms of expected values. Since $\dot{y}_s = CAx + CBu_b + CDw_b$, $\sigma_{y_s}^2$ can be written as

$$\sigma_{y_s}^2 = E\{\dot{y}_s^T \dot{y}_s\} = E\{CAx + CBu_b + CDw_b\}^T (CAx + CBu_b + CDw_b) \quad (23)$$

But $C \cdot D$ must equal zero else white noise w_w would feed through to output y_s such that $\sigma_{y_s}^2$ would be infinite (making minimization of J_{nq} meaningless). This is equivalent to saying that the transfer function relating w_w to y_s must have more poles than zeros. Expanding (23), using $\sigma_{y_s}^2$ from Eq. (18), then substituting for $\sigma_{y_s}^2$ and $\sigma_{u_b}^2$ in Eq. (20) and collecting terms, results in

$$\begin{aligned} \delta(E\{x^T(A^T C^T CA + W_1 C^T C)x\}) + \delta(E\{2x^T(A^T C^T CB)u_b\}) \\ + \delta(E\{u_b^T(B^T C^T CB + W_2)u_b\}) = 0 \quad (24) \end{aligned}$$

Now compare Eq. (24), term by term, to Eq. (22). Solving the quadratic problem with

$$\left. \begin{aligned} Q_c &= A^T C^T CA + W_1 C^T C \\ N &= A^T C^T CB \\ P_c &= B^T C^T CB + W_2 \end{aligned} \right\} \quad (25)$$

gives the desired linear controller (Kalman filter plus state estimate feedback) with one additional stipulation: At the optimum, Eqs. (21) must be satisfied. Since parameters W_1 and W_2 are functions of mean square quantities which are in turn functions of the optimal control, an iterative procedure is dictated. That is, select trial values of W_1 and W_2 and solve the quadratic problem using weighting matrices calculated using Eqs. (25). Then using the quadratic solution (in particular, X , calculated from eq. (17)), new values of W_1 and W_2 can be calculated. If these calculated values differ from the trial values, a new trial pair is selected and the quadratic problem resolved. Particular iterative techniques are discussed in Ref. 9. For the results to be presented in this paper, however, simply re-running the quadratic problem for a set of (W_1, W_2) pairs proved adequate.

One additional computation is required to calculate $\sigma_{y_s}^2$ and $\sigma_{y_s}^2$ from X , the state covariance matrix which is output from the quadratic problem. Since y_s is a scalar it can be easily shown that

$$\sigma_{y_s}^2 = CX^T C^T \quad (26)$$

and

$$\begin{aligned} \sigma_{y_s}^2 = E\{\dot{y}_s \dot{y}_s^T\} = CAXA^T C^T - 2CA(X - P)K_c^T B^T C^T \\ + CBK_c(X - P)K_c^T B^T C^T \quad (27) \end{aligned}$$

Also, the required mean square control effort can be expressed as

$$\sigma_{u_b}^2 = K_c(X - P)K_c^T \quad (28)$$

This completes the formulation of the quadratic and nonquadratic inlet problems. The next section discusses the computer algorithms used.

V COMPUTATION

The first step in the computation procedure was to solve the estimation problem, yielding a set of Kalman filter gains K_e . This step is common to both the quadratic and nonquadratic problems, as both use the same Kalman filter to generate the required state estimates.

The nonquadratic problem was handled by solving the equivalent quadratic problem for a number of trial (W_1, W_2) pairs. The solution to each quadratic problem K_c was used with the K_e previously determined to compute the mean square values of the state vector. From this, $\sigma_{y_s}^2$, σ_{y_s} , and $\sigma_{w_b}^2$ were calculated. For a range of k 's, J_{nq} , λ , W_1 , and W_2 were then calculated. All these data were scanned off-line to determine optimum points. This was done by first finding points of minimum J_{nq} for each value of k . As a check, an alternate method was used. This was to find points for constant k where the assumed W_1 was sufficiently close to the calculated W_1 and the assumed W_2 was close to the calculated W_2 . The accuracy with which the W_1 and W_2 equations (eqs. (21)) were satisfied was a function of the number of trial pairs (W_1, W_2) . That is, finding the optimum more accurately required more pairs. The quadratic problem was solved like the nonquadratic problem except only one control problem solution was required (for a given value of k).

The two major subroutines used were one for the steady-state Riccati equation and one for the steady-state covariance matrix (Lyapunov) equation. The steady-state Riccati equation subroutine used the negative exponential method.⁽¹⁰⁾ The state covariance matrix equation (eq. (17)) was solved by transforming it into a set of $n(n+1)/2$ linear equations. The solution method chosen⁽¹¹⁾ was only one of a number of possible alternate methods for solving the Lyapunov equation.

VI TRANSFER FUNCTIONS AND STATE VARIABLE MODEL

Table I shows the various transfer functions required to describe the inlet as shown in Fig. 2. G_{INLET} and G_{SHOCK} transfer functions were obtained by curve fitting unpublished NASA data. The data were taken in wind tunnel tests on the NASA 40/60 axisymmetric inlet. Data for G_{BPD} appear in Ref. 12. Note that G_{INLET} and G_{SHOCK} contain dead times. These dead times were approximated by Pade approximations in order to obtain a finite state representation. The last item in the table, G_{COLOR} , represents the available knowledge concerning the compressor face disturbance. For example, if the disturbance were generated at the upstream end, G_{COLOR} would serve to model the spectrum of atmospheric turbulence. However, for the downstream disturbance, the pole zero locations shown were chosen so that the colored disturbance is rich at low frequency (approximating a step change in engine speed), moderate at mid-frequencies (approximating combustion noise), and then cut off at high frequency. The distur-

ance spectrum of the output of this coloring circuit is arbitrary but believed to be typical of that existing at an engine compressor face.

Table II contains the necessary matrices which are used in the state variable description. These matrices were obtained using the transfer functions of table I. It can be seen in the A matrix that the first two states represent shock motion and the next four states represent inlet dynamics. The next two states are the noise coloring and the last two the bypass door dynamics. The value of measurement noise psd (r) was chosen from experience to approximate the level of noise on the throat exit static throat signal (P_{te}) found in wind tunnel tests. The psd of the white noise signal which drives the coloring circuit (q) is also arbitrary but was chosen so that the rms value of w_q is reasonable (0.168 kg/sec) compared to a nominal inlet through flow of 16.8 kg/sec.

VII RESULTS

As a basis for comparing both types of control, λ^{-1} (mean time between unstarts) was chosen as most representative of overall system performance. Since, in the performance index, the control variable was also weighted, results are shown with σ_{w_b} (bypass door flow) as a parameter. In Fig 3, λ^{-1} is plotted as a function of σ_{w_b} with α (shock position tolerance) as the parameter. The solid curves are for the quadratic case, and the dotted curves are for the nonquadratic. Both designs use identical Kalman filters. The study used only one Kalman filter, since only one Q/R ratio was considered.

The most significant point in Fig. 3 is that λ^{-1} is very sensitive to α . The value of λ^{-1} increases with both α and σ_{w_b} . For each case, each value of σ_{w_b} corresponds to a unique set of control gains (K_c), independent of α . It is apparent in Fig. 3 that both cases are quite similar in their ability to prevent unstarts for a given value of control effort. The two curves for the nonquadratic case show that this control is only slightly better than quadratic control. The basic difference between the two cases is that in the nonquadratic case $\sigma_{y_s}^2$ is weighted in addition to $\sigma_{y_s}^2$.

For each value of α , λ^{-1} is bounded, for both large and small values of σ_{w_b} . The system becomes open loop as σ_{w_b} goes to zero. The open loop values of λ^{-1} could not be shown on Fig. 3 because they are so small (for example, the open loop value of λ^{-1} is 1.5×10^{-4} hours for $\alpha = 3.44$ cm). As σ_{w_b} goes to infinity, for each value of α , λ^{-1} doesn't go to infinity (as it would were there no measurement noise), but instead reaches a limit. The limiting values of λ^{-1} could not be conveniently computed, so are not shown on Fig. 3. The best that the control can do for large σ_{w_b} is to drive the estimate of x (not x , itself) to zero.

Of the many physical constraints present in the inlet control problem, the constraint on σ_{w_b} is most important. This is because the value of σ_{w_b} dictates the capacity of the bypass doors.

This, in turn, determines the size of the bypass door actuator. A practical question is, how large can σ_{wb} be without incurring saturation on the bypass doors?

Once the actuator is selected, the other constraints must be considered. For the actuator used in these designs (described in ref. 12) there exist hard limits on bypass door velocity and acceleration. Thus, as an additional check, rms bypass door acceleration, position, and velocity were calculated. In determining how large various σ values can be without incurring saturation, the following rule-of-thumb was used: make the three σ value less than or equal to the limit value in question. Since the probability of exceeding the 3σ limit is quite small, it is then unlikely that saturation will occur. For the quadratic case the use of the limits is illustrated as follows, using limit data from Ref. 12.

Three critical values of σ_{wb} are shown on Fig. 3. Point C is the value of rms bypass door flow at which the rms bypass door position is equal to one third of its maximum (full open) value. If no other constraints existed, feasible optimal controllers would be all those producing rms bypass door flow rates less than or equal to 5.6 kg/sec (point C). However, when velocity and acceleration constraints on the bypass doors are considered, the only feasible controllers are those which have rms bypass door flow rates less than or equal to 0.091 kg/sec (point A). Point A indicates the value of σ_{wb} (and corresponding optimal controller) for which the rms bypass door acceleration is equal to one-third of its hard limit (maximum) value. Note that the velocity limit (point B) lies between points A and C, thus it is not the determining factor in controller selection. A more general approach to the actuator saturation problem would have been to weigh, in the performance index, in addition to bypass door input, bypass door flow rate and rate of change of flow rate (both of which are state variables). This, however, was not done in this study.

Controls are also compared on a closed loop frequency response basis. Figure 4 shows closed loop frequency responses for shock-position-to-compressor face flow disturbance. Note again the similarity between quadratic and nonquadratic designs. The fact that the colored noise w_d had an appreciable amplitude in the mid frequency range caused the closed loop to stay under the open loop until about 70 Hz. Zero frequency disturbances are attenuated by about two orders of magnitude. Referring to Fig. 3, for the levels of control effort selected, it can be seen that small changes in the frequency response magnitude (fig. 4) correspond to large changes in λ^{-1} . This again demonstrates the difficulty in using λ alone as the performance criterion - it is very sensitive to small changes in controller parameters.

In addition to closed loop analyses, the Kalman filter-plus-control gain combinations were examined as conventional controllers. Figure 5 shows the open loop frequency response of bypass door command voltage to a change in throat exit static pressure (transfer function $G_{CONTROL}$ in fig. 2).

This corresponds to the feedback compensator of classical control design. Again, quadratic designs are seen to be very similar to nonquadratic designs (for the same value of rms bypass flow). It should be noted here that the inlet is uncontrollable, but that the uncontrollability creates no problem with any of the computer algorithms. In particular, it can be seen in table I that the 500 rad/sec pole in G_{SHOCK} is uncontrollable, as are the two noise coloring poles. Since all are stable, the uncontrollability creates no problems.

The controller represented in Fig. 5 is tenth order. Since a tenth order control is possibly more complex than desired, simplification techniques were investigated. One method of simplification would be to curve fit the data on Fig. 5 with a model of desired order. A better approach to simplification would be to apply a general simplification technique (for example, as shown in ref. 13) to the controller. For this problem, it turned out that basic simplifications could be made just by examining the controller root locus. Two pole zero cancellations and one near cancellation can be seen on Fig. 6. Figure 6 was plotted as a root locus of the controllers for the quadratic case. It was made by taking the eigenvalues of $(A - BK_c - K_eH)$ and zeros of $K_c(sI - (A - BK_c - K_eH))^{-1}K_e$. The parameter on the loci is σ_{wb} . Of the ten poles and nine zeros shown, three cancellations occur. In particular, the two thousand rad/sec noise coloring pole is almost cancelled in addition to the 800 rad/sec and 500 rad/sec shock position poles which are exactly cancelled. Thus, the controller can be implemented as a 6th/7th order system. It's possible, of course, that further simplifications could be made and results of the simplifications evaluated by recomputing J_q .

VIII CONCLUSIONS

It was found that through the use of the quadratic equivalence principle, a control was designed which minimized a physically meaningful performance index. The control system resulting is the best linear control which minimizes the nonquadratic index. The particular nonquadratic index used was quite sensitive to shock position tolerance. It was found that using a quadratic index (minimizing shock position deviation) gave results very similar to the nonquadratic results. Since the quadratic approach requires only one computation of the Riccati equation for each controller, while the nonquadratic requires several, the simpler quadratic approach may still be more attractive. While the example in this study was a single-input, single-output case, the methods could be extended to the more realistic inlet problem, including atmospheric turbulence disturbance, centerbody actuation for throat Mach number control, and compressor face or other additional pressure measurements.

IX REFERENCES

- (1) Walitt, L., "On the Dynamics of a Supercritical Inlet," M.S. Thesis, University of California, Los Angeles (1962).

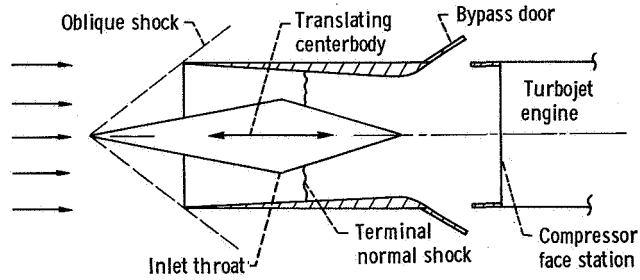


Figure 1. - Schematic of supersonic axisymmetric inlet.

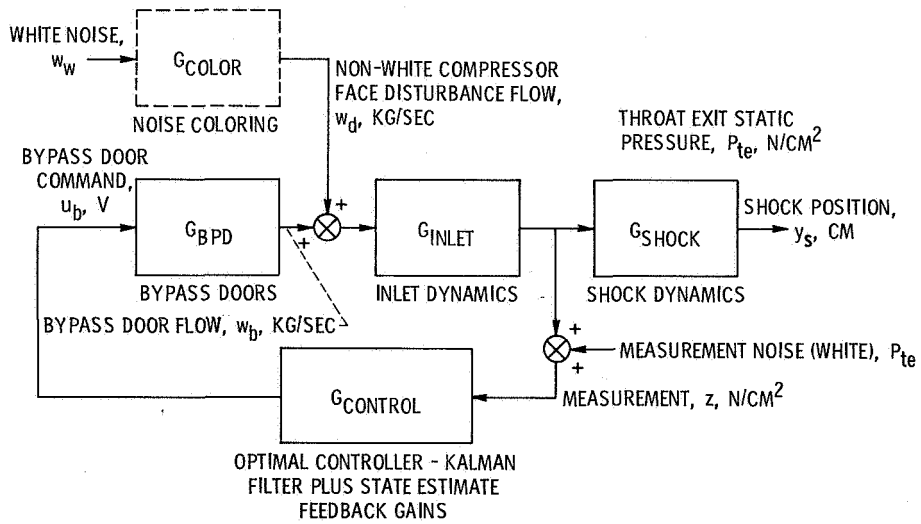


Figure 2. - Inlet control system block diagram.

ACTUATOR LIMITS, QUADRATIC CASE

- A RMS BYPASS DOOR ACCELERATION
= 1/3 OF HARD LIMIT
- B RMS BYPASS DOOR VELOCITY
= 1/3 OF HARD LIMIT
- C RMS BYPASS DOOR POSITION
= 1/3 OF HARD LIMIT

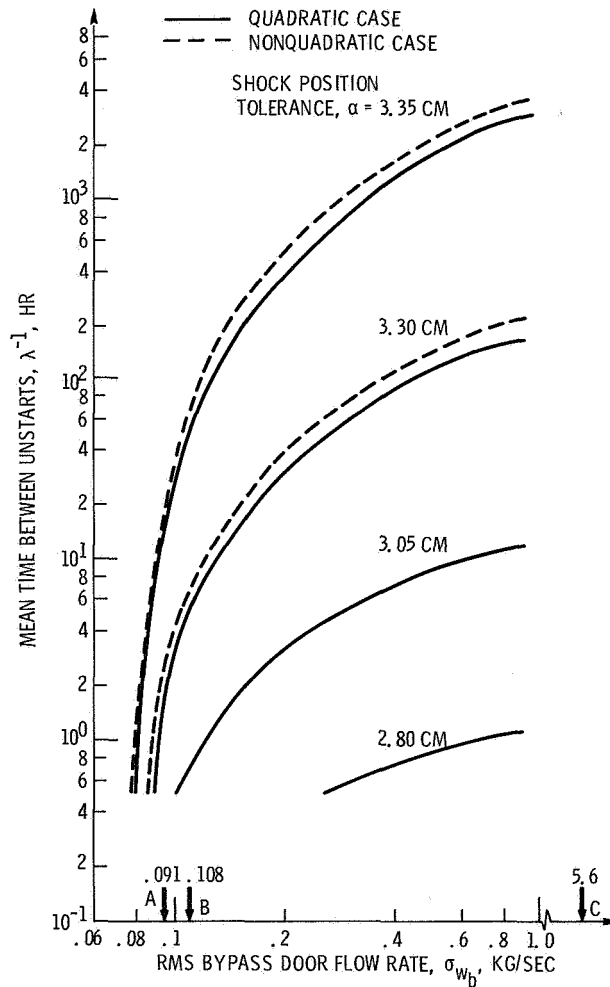


Figure 3. - Mean time between unstarts as a function of RMS bypass door flow rate, quadratic and nonquadratic case.

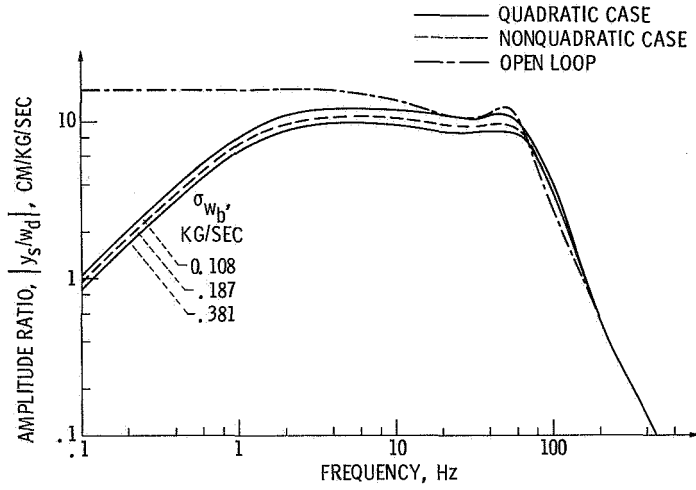


Figure 4. - Closed loop frequency responses, quadratic and nonquadratic cases, shock position to compressor face flow disturbance.

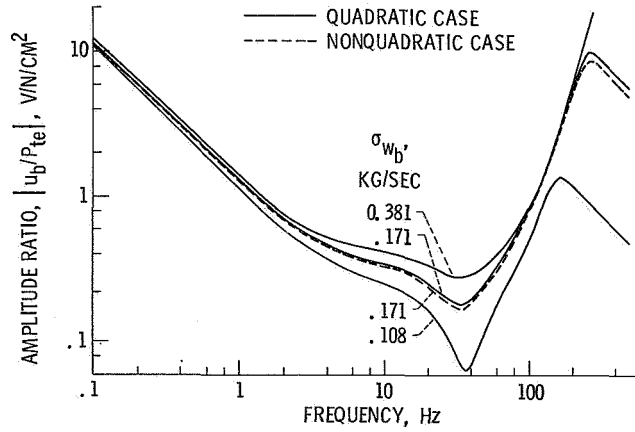


Figure 5. - Controller frequency responses, quadratic, and nonquadratic cases, bypass door command voltage to throat exit static pressure.

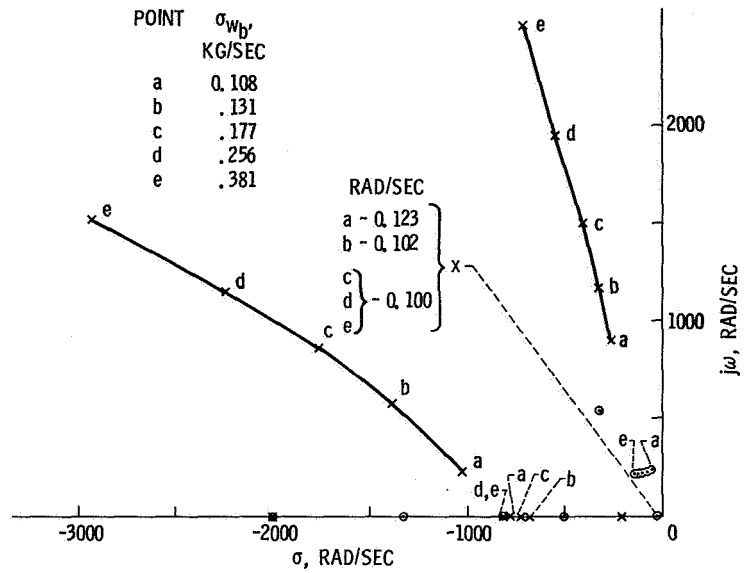


Figure 6. - Controller root locus for quadratic case with σ_{wb} as the parameter.